International Journal of Nanomedicine

Dovepress
open access to scientific and medical research

Open Access Full Text Article

ORIGINAL RESEARCH

Pharmacokinetics and enhanced oral bioavailability in beagle dogs of cyclosporine A encapsulated in glyceryl monooleate/poloxamer 407 cubic nanoparticles

This article was published in the following Dove Press journal:
International Journal of Nanomedicine
16 December 2009
Number of times this article has been viewed

Jie Lai[1,2]
Yi Lu[1]
Zongning Yin[2]
Fuqiang Hu[3]
Wei Wu[1]

[1]School of Pharmacy, Fudan University, Shanghai, China, [2]West China School of Pharmacy, Sichuan University, Chengdu, China, [3]School of Pharmacy, Zhejiang University, Hangzhou, China

Abstract: Efforts to improve the oral bioavailability of cyclosporine A (CyA) remains a challenge in the field of drug delivery. In this study, glyceryl monooleate (GMO)/poloxamer 407 cubic nanoparticles were evaluated as potential vehicles to improve the oral bioavailability of CyA. Cubic nanoparticles were prepared via the fragmentation of a bulk GMO/poloxamer 407 cubic phase gel by sonication and homogenization. The cubic inner structure formed was verified using Cryo-TEM. The mean diameters of the nanoparticles were about 180 nm, and the entrapment efficiency of these particles for CyA was over 85%. The *in vitro* release of CyA from these nanoparticles was less than 5% at 12 h. The results of a pharmacokinetic study in beagle dogs showed improved absorption of CyA from cubic nanoparticles as compared to microemulsion-based Neoral®; higher C_{max} (1371.18 ± 37.34 vs 969.68 ± 176.3 ng mL^{-1}), higher AUC_{0-t} (7757.21 ± 1093.64 vs 4739.52 ± 806.30 ng h mL^{-1}) and $AUC_{0-\infty}$ (9004.77 ± 1090.38 vs 5462.31 ± 930.76 ng h mL^{-1}). The relative oral bioavailability of CyA cubic nanoparticles calculated on the basis of $AUC_{0-\infty}$ was about 178% as compared to Neoral®. The enhanced bioavailability of CyA is likely due to facilitated absorption by cubic nanoparticles rather than improved release.

Keywords: nanoparticles, cubosomes, cyclosporine A, glyceryl monooleate, oral drug delivery, bioavailability, beagle dogs

Introduction

Cyclosporine A (CyA) is a potent cyclic polypeptide immunosuppressant and has been used clinically to prevent allograft rejection in various organ transplantations and to treat systemic and local autoimmune disorders.[1] Although CyA is clinically successful, its oral absorption remains limited due to its high lipophilicity, low intestinal permeability,[2] P-glycoprotein (P-gp) efflux from the enterocytes and extensive pre-systemic metabolism in the gut wall and liver.[3] CyA was originally formulated as an oily solution (Sandimmun®), but was found to have high variability in its oral bioavailability of between 1% and 89%.[4,5] The first-class dosage form of CyA that is now used clinically is a self-microemulsifying concentrate (Neoral®) that shows a 70% to 135% increase in C_{max} and *AUC* in volunteers[6] as compared to the oily solution. Efforts are still being made to improve the oral bioavailability of CyA to optimize its *in vivo* performance.

To date, comparable or increased bioavailability of CyA as compared to Neoral® has been achieved by using a series of vehicles including pH-sensitive nanoparticles,[7–9]

Correspondence: Wei Wu
School of Pharmacy, Fudan University, 826 Zhangheng Road, Shanghai 201203, China
Tel +86 21 5198 0002
Fax +86 21 5198 0002
Email wuwei@shmu.edu.cn

Zongning Yin
West China School of Pharmacy, Sichuan University 610041, China
Tel +86 28 8950 2917
Fax +86 28 8550 2917
Email yzn@scu.edu.cn

poly (lactic acid-co-glycolic acid) (PLGA) nanoparticles,[10] positively charged chitosan and gelatin nanoparticles,[11] solid lipid nanoparticles,[12] polymeric micelles,[13] sodium cholate/lecithin mixed micelles,[14] sodium lauryl sulfate-dextrin based solid microspheres,[15] liposomes[16] and proliposomes,[17] solid dispersion containing polyoxyethylene (40) stearate,[18] artificial oil bodies stabilized by caleosi[19] and O/W-emulsion.[20] Unfortunately, by simply enhancing the dissolution of CyA from the vehicles may not lead to increased oral bioavailability of CyA.[18] Therefore, new vehicles are required to improve dissolution and permeation simultaneously to improve oral bioavailability of CyA. Lyotropic vehicles based on lipids are able to maintain drugs in a solubilized state in the gastrointestinal (GI) tract and penetrate the "unstirred water layer" with ease.[21] Most importantly, lipid-based drug delivery systems are able to transform into important secondary vehicles (mixed micelles, cubic and hexagonal nanoparticles, vesicular carriers) in the GI and are believed to facilitate absorption of lipids and poorly water-soluble drugs.[22]

Cubic nanoparticles (cubosomes) are dispersions of cubic phases composed of lipid bilayers partitioning into bicontinuous contortions of inter-connecting hydrophilic and hydrophobic domains.[23,24] The unique structure and properties of cubic nanoparticles endowed them with special interest as drug delivery carriers.[25,26] However, their potential as oral drug delivery vehicles has not been extensively explored. Preliminary results showed enhanced oral absorption of insulin by glyceryl monooleate (GMO)/poloxamer 407 cubic nanoparticles.[27,28] To date, cubic nanoparticles have not been well studied for oral delivery of poorly water-soluble drugs. Being largely different in physicochemical properties, poorly water-soluble drugs in cubic nanoparticles will have different fate in the GI tract from water-soluble drugs like insulin. For the following reasons, cubic nanoparticles seem to be advantageous as oral delivery carriers for poorly water-soluble drugs. Firstly, being lyotropic,[23,24] cubic nanoparticles can hold poorly water-soluble drugs in their lipid bilayers in a solubilized state. Most importantly, since the cubic phase is isotropic, the solubilized state can be retained, without concern of drug precipitation in the GI tract, after cubic nanoparticles have been broken down into smaller particles during the digestion process by the intestinal lipases. Secondly, the cubic nanoparticles are bioadhesive,[26] which increases the opportunities of close contact of drug-loaded nanoparticles with intestinal cell membrane. Thirdly, as a secondary vehicle during lipid digestion, cubic nanoparticles are assumed to play important roles in the process of lipid and drug absorption.[22] Since permeation enhancement by cubic phases has been observed for transdermal and transmucosal delivery,[25,26] similar mechanisms may be proposed for cubic nanoparticles as oral delivery carriers.

In a previous study,[29] enhanced oral bioavailability of simvastatin, a BCS II drug, has been achieved by GMO/poloxamer 407 cubic nanoparticles. Taking advantage of their permeation-enhancing effect, cubic nanoparticles were evaluated as potential vehicles to improve the oral bioavailability of CyA, a more challenging BCS IV drug of poor water-solubility and poor permeability.

Materials and methods

Materials

Cyclosporine A (CyA) was purchased from Pharmaceutical Factory of Sichuan Institute of Antibiotic Industries (Chengdu, China). Glyceryl monooleate (monoolein, GMO) DIMONANR MO 90/D was a gift from Danisco Cultor (Grindsted, Denmark). Poloxamer 407 (PEO98POP67PEO98) was provided by BASF (Ludwigshafen, Germany). Sephadex G-50 was purchased from Pharmacia. Water was prepared by Millipore purifying system (Molsheim, France). HPLC-grade methanol was supplied by Merck (Darmstadt, Germany). All other chemicals used in the study were of analytical grade.

Preparation of CyA-loaded GMO/poloxamer 407 cubic nanoparticles

Cubic nanoparticles were prepared through the fragmentation of GMO/poloxamer 407 bulk cubic gel.[30] GMO (500 mg) and poloxamer 407 in various weight (40–100 mg) were firstly melted at 60°C in a hot water bath, after which CyA was added and stirred continuously to dissolve. Milli-Q deionized water (250 μL) was added gradually and vortex mixed to achieve a homogenous state. After equilibration for 48 h at room temperature, an optically isotropic cubic phase gel formed. After addition of 10 mL deionized water, the cubic gel was first disrupted by mechanical stirring. The crude dispersion was subsequently fragmented by intermittent probe sonication at 200 W energy input (JYD-650, Shanghai, China) under cooling in a 20°C water bath for 10 min, and homogenized by passing five cycles through a high-pressure homogenizer (Avestin Em-C3, Ottawa, Canada) at 670 bar and 25°C to obtain an opalescent dispersion of the cubic nanoparticles. The final dispersions of cubic nanoparticles were stored at room temperature until required.

For preparation of samples for release and pharmacokinetic studies, the crude dispersions of tens of repeats were pooled and further processed under the conditions described above to obtain the fine dispersion of CyA-loaded

GMO/poloxamer 407 cubic nanoparticles. The free drug was removed by eluting through a Sephadex G-50 column following the procedures similar to those described below for the determination of entrapment efficiency. The formulation details and fundamental properties of the cubic nanoparticle dispersion were listed in Table 1.

Characterization of CyA-GMO/poloxamer 407 cubic nanoparticles

The inner cubic structure of the nanoparticles was characterized by Cryo-TEM (JOEL JEM-2010, Tokyo, Japan). A thin liquid film of nanoparticles (20–400 nm) was prepared on a copper grid and then immersed into liquid ethane. Excess ethane was removed, and the sample was transferred into a Cryo-TEM. Samples were viewed under low-dose conditions at a constant temperature of –170°C. All images were recorded digitally with a CCD camera (Gatan 832) under low-dose conditions with an underfocus of approximately 3 μm and acceleration voltage of 120 kV.

Particle size was determined by photon correlation spectroscopy using a Zetasizer Nano® (Malvern Instruments, Malvern, UK) equipped with a 4 mW He–Ne laser (633 nm) at 25°C. Samples were diluted with deionized water prior to measurement, setting dispersant viscosity to 0.8872 cP at 25°C.

For determination of entrapment efficiency, it was mandated to separate free CyA from nanoparticle-associated CyA. Gel permeation chromatography was one of such separating method commonly used.[31,32] In this study, the entrapment efficiency of CyA was measured by gel permeation chromatography using Sephadex G-50. CyA-loaded cubic nanoparticles were eluted through Sephadex G-50 (2 g) columns (ϕ1.5 cm × 30 cm) after preconditioning with 30 mL water. Cubic nanoparticles were separated from free CyA by monitoring turbidity at a wavelength of 500 nm by a UV-2401 spectrophotometer (Shimadzu, Tokyo, Japan). Good column recoveries of 98%–101% were observed. Free and associated CyA were determined by HPLC at 226 nm. The LC-10ATvp HPLC system (Shimadzu) was composed of a binary pump, a tunable ultraviolet detector, a column heater and a manual injector. The mobile phase, pumped at a flow rate of 1.0 mL min^{-1}, consisted of an acetonitrile/water/*tert*-butylmethylether/phosphoric acid (600/350/50/1, v/v/v/v) mixture. CyA was separated using a C18 column (Venusil XBP, 5 μm, 4.6 mm × 150 mm; Agela, Tianjin, China) guarded with a refillable precolumn (C18, 2.0 mm × 20 mm; Alltech, Lexington, KY, USA) and a stainless pre-heating tube 1000 mm in length with an internal diameter of 0.25 mm maintained at 70°C. The linearity range of the calibration curve was within 1.0–15 μg mL^{-1} with a correlation coefficient of 0.9997 ± 0.0002. Entrapment efficiency (*EE*%) was calculated as $W_c/W_t \times 100\%$, where W_c and W_t denote CyA content in cubic nanoparticles and total drug in dispersion.

Release of CyA from cubic nanoparticles

A preliminary study on CyA release from the cubic nanoparticles of the same formulation as for the further pharmacokinetic study (Table 1) was carried out using the dynamic dialysis method in a ZRS-8G release tester (Tianjin, China). Two milliliters CyA-loaded cubic nanoparticles (4 mg CyA equivalent) were sealed in dialysis bags (14000 MWCO, Millipore, Boston, MA, USA) and immersed in 100 mL aqueous medium containing 0.2% (w/v) sodium lauryl sulfate (SDS) thermostatically maintained at 37 ± 0.5°C and stirred at a revolution speed of 100 rpm. At time intervals of 0.25, 0.50, 0.75, 1.0, 2.0, 3.0, 4.0, 5.0, 6.0, 8.0, 10, and 12 h, 0.2 mL of medium was withdrawn and filter through a 0.45 μm nylon film. The CyA content was then determined by HPLC as described above. Since the solubility of CyA in 0.2% SDS solution was about 0.921 mg/mL, the sink conditions were maintained throughout the release test. Nearly complete release within 1 h was observed for saturated CyA solution indicating negligible hindering effect of the dialysis bag on CyA release.

Determination of CyA in dog whole blood by RP-HPLC

CyA in dog whole blood was determined using our HPLC-UV method as described above with minor modification. The same LC-10ATvp HPLC system and Venusil XBP C18 column with guard column and pre-heating assemblies as in entrapment efficiency determination was used. The mobile phase was composed of acetonitrile/water/

Table 1 Formulation details and properties of CyA-loaded cubic nanoparticles

Poloxamer 407/GMO ratio	Theoretical solid content (%, w/v)[a]	Theoretical drug loading (%)[b]	Particle size (nm)	Polydispersity	Entrapment efficiency (%)
12/100	11.4	1.75	136.4 ± 5.8	0.291	91.45 ± 1.45

Notes: [a]Calculated as the weight ratio of (GMO + poloxamer 407) to total sample (GMO + poloxamer 407 + water); [b]Calculated as the weight ratio of CyA to total solids (CyA + GMO + poloxamer 407).

tert-butylmethylether/phosphoric acid (525/425/50/1, v/v/v/v) and run at a flow rate of 1.5 mL min^{-1}. CyA was measured at 210 nm.

To prepare dog blood samples, CyA was extracted by the reported liquid-liquid extraction procedures[7,33] with minor modification. To 2 mL dog blood, add 100 mg of sodium fluoride followed by 160 µL of internal standard solution (cyclosporine D, 10 µg mL^{-1} in methanol). After vortex mixing for 30 s, 5 mL of diethyl ether anhydrous was added and vortex mixed for 10 min. After centrifuging at 2000 × g for 10 min, the organic layer was transferred to another tube and evaporated under a light stream of nitrogen at 40°C. The residue was reconstituted using 120 µL methanol/0.05 mol L^{-1} hydrochloric acid solution (6/4, v/v). After washing the injection solution with 1 mL *n*-hexane for 2 min and a brief centrifugation at 2000 × g for 10 min, 20 µL of the injection solution was injected for HPLC analysis. Quantification was based on the peak area ratio R (A_{CyA}/A_{IS}). Linearity was observed over the concentration range of 25–2000 ng mL^{-1} with correlation coefficients of over 0.99 (a typical calibration curve: $R = 0.003C–0.0842$, ($r = 0.9976$, $n = 7$). The lower limit of quantification (LLOQ) for the determination of CyA in dog plasma was found to be 12.1 ng mL^{-1}. Accuracy for the determination of CyA in dog plasma ($n = 9$) was 94.58 ± 3.06%. Intra-day and inter-day precisions were below 7% and the extraction recovery of CyA in dog plasma ($n = 9$) was 74.36 ± 3.44%.

Bioavailability study

The pharmacokinetics of the CyA cubic nanoparticle dispersion (Table 1) was compared with a CyA capsule (25 mg/capsule, Sandimmun Neoral®, Novartis) in beagle dogs in a randomized two-period crossover study after an oral dose of 100 mg equivalent CyA. The particle size of Neoral® was 14.3 ± 4.52 nm determined by Zetasizer Nano® under conditions in this study after diluting its content with 25 mL deionized water. The washout period between administrations was one week. Six male beagle dogs weighing 8–10 kg were kept in an environmentally controlled breeding room (22 ± 2°C, 60 ± 5% relative humidity, fresh air circulating) for one week before the start of the experiment. The dogs were fed standard laboratory chow with water and fasted overnight before the experiment. Guidelines on experiments involving use of animals were issued by the Ethical Committee of Fudan University in adherence to MOH guidelines (Ministry of Health of the People's Republic of China Publication, 1998). The cubic nanoparticle dispersion was gavage administered, whereas the Neoral capsules were put at the pharyngeal site and swallowed spontaneously by the animals, followed by flushing with 20 mL of water. After administration, about 4 mL of blood was collected through the hind leg vein into heparinized tubes at time intervals of 0.5, 1.0, 1.5, 2.0, 2.5, 3.0, 4.0, 6.0, 8.0, 12.0, and 24.0 h. Blood samples were stored at −20°C until analysis.

Pharmacokinetic analysis was performed by a model-independent method and a two-compartmental method, respectively, using the 3P87 computer program (issued by the State Food and Drug Administration of China for pharmacokinetic study). C_{max} and T_{max} were observed as raw data. Area under the curve to the last measurable concentration (AUC_{0-t}) was calculated by the linear trapezoidal rule. Area under the curve extrapolated to infinity ($AUC_{0-\infty}$) was calculated as $AUC_{0-t} + C_t/k$, where C_t and k were the last measurable concentration and the elimination constant, respectively.

Statistical analysis

Raw data were analyzed using the SPSS statistical software (version 11.0, SPSS, Inc., Chicago, IL, USA). Post-hoc multiple comparisons were done using one-way ANOVA and the Student–Newman–Keuls test (q test) to determine the significance of differences between groups; a P value less than 0.05 was considered statistically significant.

Results and discussion

Preparation and characterization of CyA-GMO/poloxamer 407 cubic nanoparticles

Clear and viscous gels were formed using the GMO/poloxamer 407 binary systems with a GMO/poloxamer 407 ratio of 500 mg/40 mg (7.4%, w/w, poloxamer 407 weight percentage) to 500 mg/100 mg (16.7%, w/w). Analysis of each preparation using polarized light microscopy indicated that the diffraction of a dark isotropy indicated the formation of the liquid crystalline phase. At lower CyA loading, no significant change in the appearance of the bulk gel was observed. However, when the theoretical CyA loading increased to over 2% (w/w), calculated as the ratio of CyA to total solids, the bulk gel began to turn opalescent indicating reduced solubility of CyA in the GMO/poloxamer 407 cubic phase. The theoretical CyA loading was fixed at 1.75% in all preliminary studies.

Cryo-TEM revealed the inner structure of the blank (Figure 1A) and CyA-loaded (Figure 1B) GMO/poloxamer 407 cubic nanoparticles, whose formulation details and properties are listed in Table 1. Typical cubic structures indicating the formation of cubic nanoparticles were confirmed; nanoparticles of larger diameters had bulk cubic geometry,

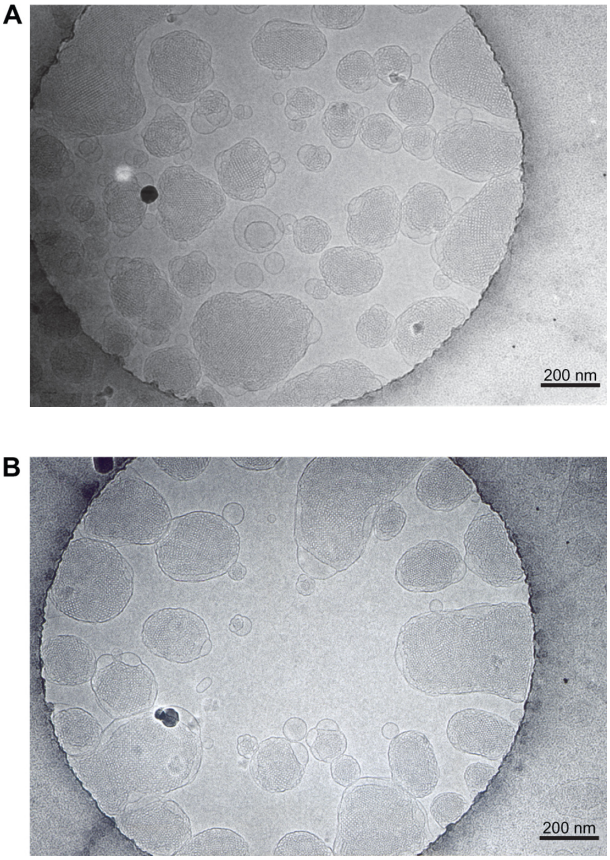

Figure 1 Cryo-TEM photographs of blank **A**) and CyA-loaded **B**) cubic nanoparticles. The bars equal 200 nm.

while those of smaller diameters showed oval or spherical geometry. CyA loading at 1.75% (w/w) seemed to have little effect on the cubic structure of the nanoparticles.

During the sonication procedure, the cubic phase gel was efficiently disrupted. Particle size analysis gave a mean diameter of 200–300 nm and a wide particle size distribution ranging from 30 nm to 1000 nm (Figure 2A). After homogenization, the mean diameter of the particles was reduced to about 180 nm with a narrower lognormal size distribution within 70–300 nm (Figure 2B). The GMO/poloxamer 407 ratio had no significant effect ($P < 0.05$) on the particle size except at the ratio of 100/20 (Figure 3A). Increasing the homogenization pressure to 670 bar could efficiently reduce the particle size (Figure 3B) as a result of increased energy input, whereas the homogenization cycles, either three or five, appeared to have no significant effect on particle size except at 350 bar (Figure 3B). It seems that homogenization was more efficient at higher pressure and three homogenization cycles were enough to obtain stable particle size, while at lower pressures more homogenization cycles were needed to obtain cubic nanoparticles of smaller diameters. Under the homogenization conditions in this study, cubic nanoparticles with reproducible particle size and distribution could be obtained.

The entrapment efficiency of CyA into cubic nanoparticles was found to be exclusively high for all formulations although the formulation variables and processing conditions had definite influence on entrapment efficiency. Under different GMO/poloxamer 407 ratios, the entrapment efficiency was between 86.2%–92.4% and showed minimal loss into the dispersion medium (Figure 4A). Highest entrapment efficiency was achieved at GMO/poloxamer 407 ratio of 100/9, which was significantly different from those obtained at other GMO/poloxamer 407 ratios ($P < 0.05$). At GMO/poloxamer 407 ratios of 100/15 and 100/20, the entrapment efficiencies were similar and significantly lower than those obtained at other GMO/poloxamer 407 ratios ($P < 0.05$). Poloxamer 407 seemed to facilitate solubilization of CyA in GMO/poloxamer 407 cubic structure at lower levels, which reached a peak at GMO/poloxamer 407 ratio of 100/9. However, when the content of poloxamer 407 increased to much high level, the ability of the cubic structure to hold CyA decreased possibly due to the increased hydrophilicity of the cubic structure and escape of CyA into the outer aqueous environment together with poloxamer 407. Homogenization pressure and cycles appeared to have no significant effect on entrapment efficiency except that significant difference ($P < 0.05$) was observed for three and five homogenization cycles at 670 bar (Figure 4B). The high entrapment efficiency may be ascribed to the high hydrophobicity of CyA and its relatively large molecule size.

The high affinity of CyA with the hydrophobic domain in the cubic phase made it difficult to be released from the nanoparticles. As a result, the overall release of CyA from cubic nanoparticles was less than 5% at 12 h (Figure 5). Similarly, release of CyA from microemulsion (Sandimmun Neoral®) was less than 5% at 12 h too. Since the overall release of CyA from cubic nanoparticles was negligible, we did not take out extensive study on release of other formulations in this study.

Pharmacokinetics and oral bioavailability

The oral bioavailability of CyA from cubic nanoparticle was assessed in beagle dogs and compared to Sandimmun Neoral®. Figure 6 shows the mean CyA plasma concentration versus time plots of the two CyA formulations. The pharmacokinetic parameters obtained using the noncompartmental method and two-compartmental method are given in Table 2 and 3.

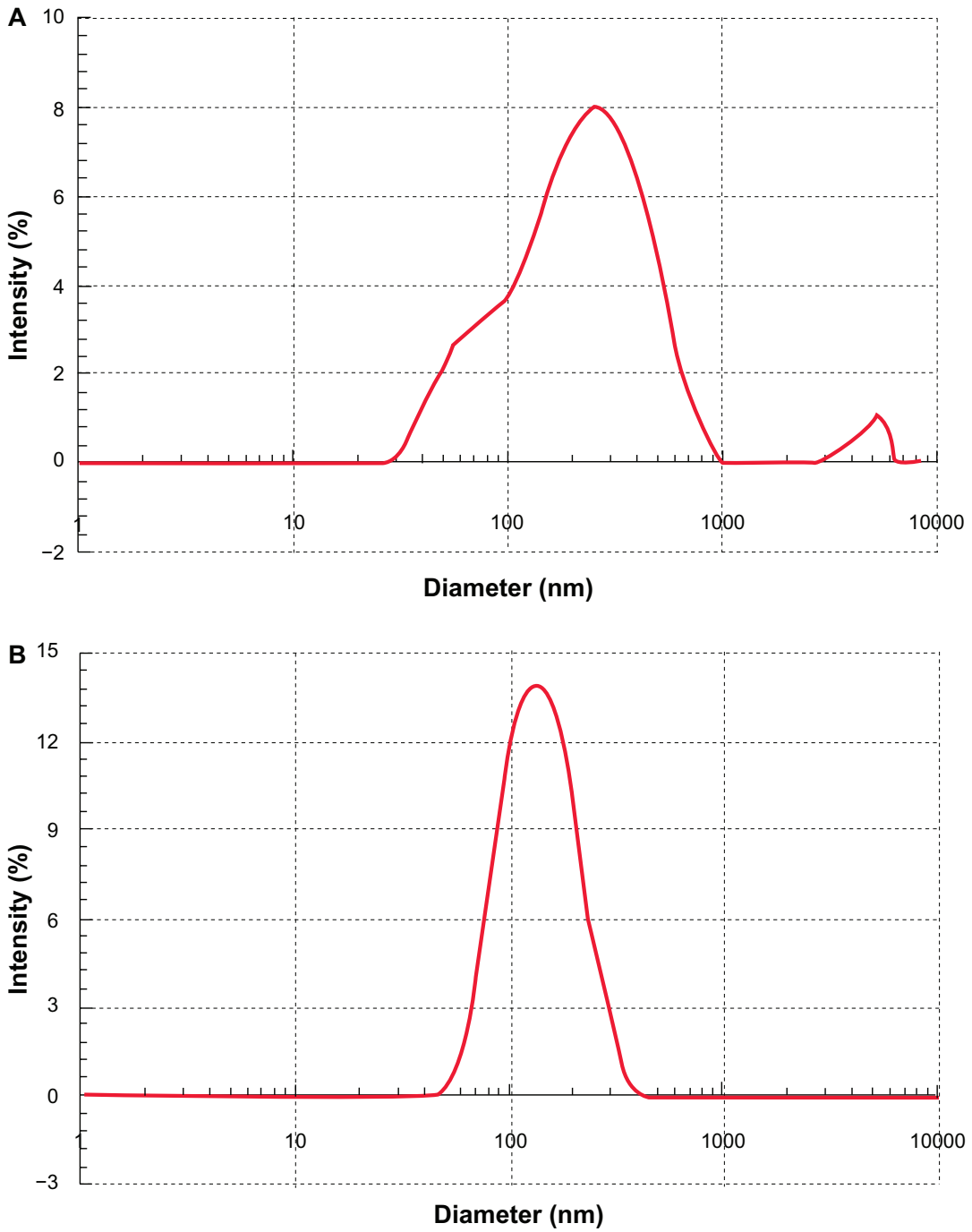

Figure 2 Size distribution of CyA-loaded cubic nanoparticles after sonication **A**) and homogenization at 689 bar for five cycles **B**).

The noncompartmental calculation indicated that the T_{max} of cubic nanoparticles (2.42 ± 0.80 h) appeared to be longer than that for Neoral® (2.00 ± 0.71 h) but, was not significantly different ($P > 0.05$). However, the C_{max} of cubic nanoparticles (1371.18 ± 357.34 ng mL^{-1}) was significantly different from that of Neoral® (969.68 ± 176.3 ng mL^{-1}) ($P < 0.05$). Cubic nanoparticles had a faster elimination rate with a smaller $t_{1/2}$ (12.14 ± 8.37 h) than Neoral® (22.29 ± 10.54 h) ($P < 0.05$). Both the AUC_{0-t} (7757.21 ± 1093.64 vs 4739.52 ± 806.30 ng h mL^{-1}) and $AUC_{0-\infty}$ (9004.77 ± 1090.38 vs 5462.31 ± 930.76 ng h mL^{-1}) were significantly different when comparing the two formulations ($P < 0.05$). Indeed, calculated on the basis of the $AUC_{0-\infty}$ of each formulation, the oral bioavailability of CyA-loaded GMO/poloxamer 407 cubic nanoparticles was about 178% as compared to Sandimmun Neoral®.

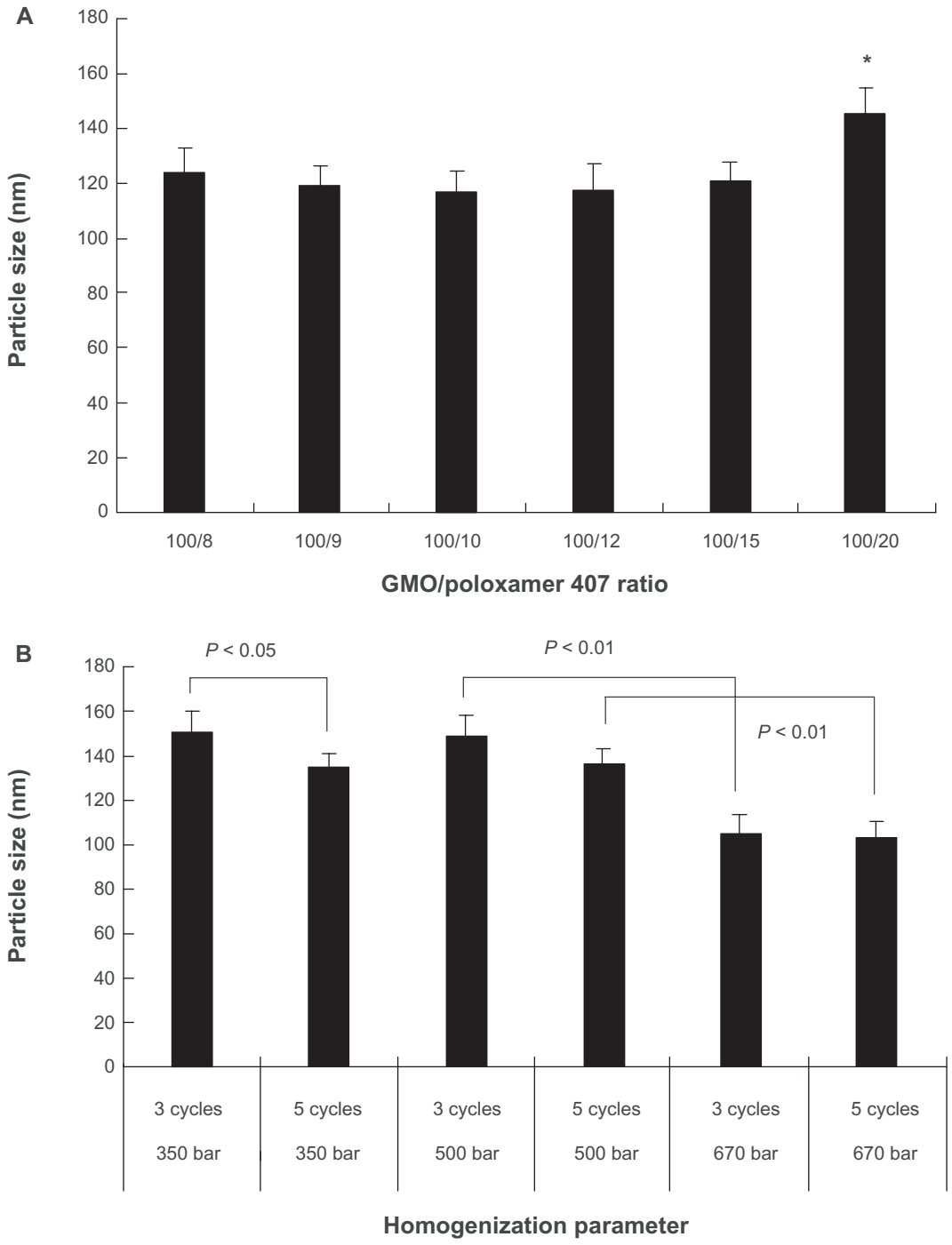

Figure 3 Effect of GMO/poloxamer 407 ratio **A**) and homogenization pressure and cycles **B**) on mean diameter of CyA-loaded cubic nanoparticles ($n = 3$).
Note: *$P < 0.01$ compared to any other group.

A two-compartmental model can be employed to fit the experimental data of both CyA cubic nanoparticles and Sandimmun Neoral® with regression coefficients of 0.9747 and 0.9901, respectively. The absorption rates of the two formulations were similar with $t_{1/2(a)}$ of 1.46 ± 0.37 h and 1.14 ± 0.61 h for cubic nanoparticles and Neoral®, respectively. The elimination from the central compartment (k_{10}) showed no significant difference ($P > 0.05$), while transportation from the central to the peripheral compartment (k_{12}) of cubic nanoparticles was faster than Neoral® ($P < 0.05$). No significant differences were observed for the transportation of CyA from peripheral to the central compartment (k_{21}) ($P > 0.05$). Distribution ($t_{1/2(\alpha)}$) of CyA after cubic nanoparticles administration was slower than Neoral® ($P < 0.05$)

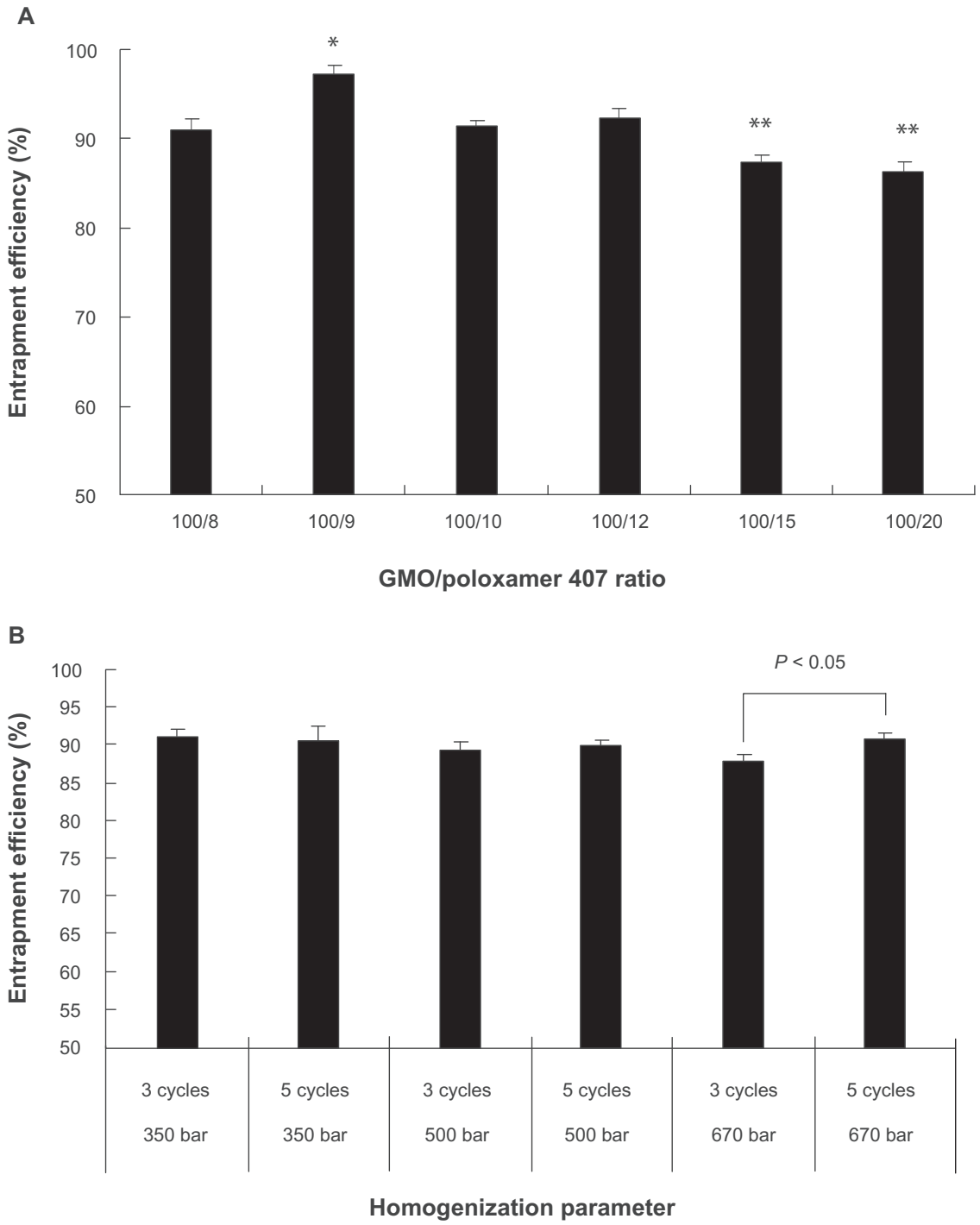

Figure 4 Effect of GMO/poloxamer 407 ratios **A**) and homogenization pressure and cycles **B**) on entrapment efficiency of CyA-loaded cubic nanoparticles ($n = 3$).
Notes: *$P < 0.05$ as compared to any other group; **$P < 0.05$ as compared to any other group except these two groups.

although the overall elimination of CyA cubic nanoparticles was faster. Indeed, plasma CyA was maintained at a high level for a longer period as compared to Neoral®. This observation may be ascribable to the enhanced absorption of CyA from cubic nanoparticles. The pharmacokinetic parameters of Neoral® reported in this study differ from that reported by Guo and colleagues[16] possibly due to the fact that we are using a beagle dog model rather than a rabbit model. The results in this study showed smaller α, β, K_a, K_{10}, K_{12} and K_{21} values and larger $T_{1/2(a)}$, $T_{1/2(\alpha)}$ and $T_{1/2(\beta)}$ values, indicating slower absorption, distribution, transportation between compartments and elimination in beagle dogs than in rabbits.

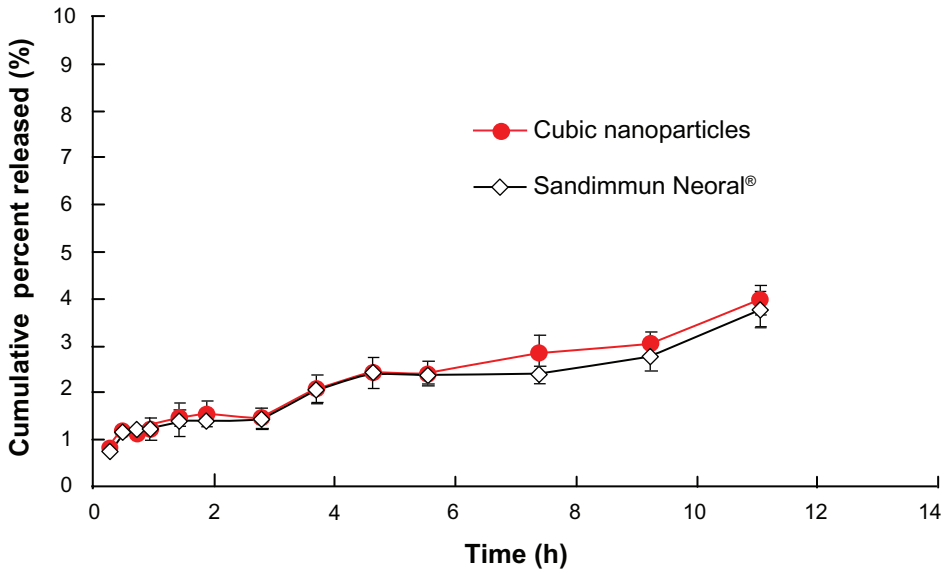

Figure 5 Release profiles of CyA-loaded GMO/poloxamer 407 cubic nanoparticles and Neoral® capsules ($n = 3$).

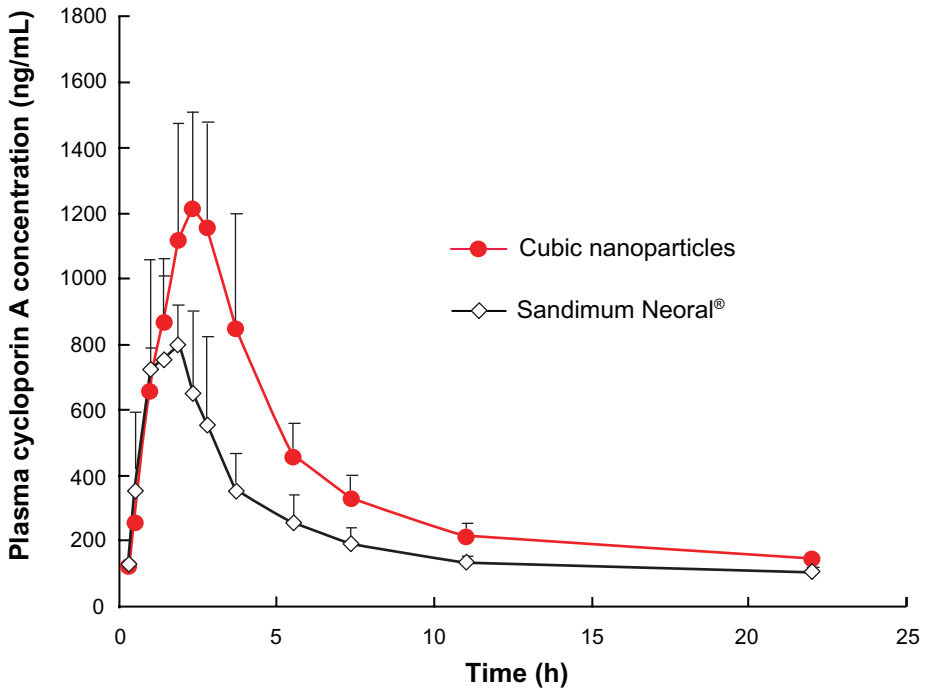

Figure 6 Beagle dog plasma CyA concentrations versus time plot after a single oral dose of 100 mg equivalent CyA cubic nanoparticles or Sandimmun Neoral® ($n = 6$).

Table 2 Pharmacokinetic parameters after oral administration of CyA-loaded cubic nanoparticles and Sandimmun Neoral® calculated by a noncompartmental method

Formulation	t_{max} (h)	C_{max} (ng mL^{-1})	$t_{1/2}$ (h)	AUC_{0-t} (ng h mL^{-1})	$AUC_{0-\infty}$ (ng h mL^{-1})	*MRT* (h)	Relative bioavailability (%)*
Cubic nanoparticles	2.42 ± 0.80	1371.18 ± 357.34	12.14 ± 8.37	7757.21 ± 1093.64	9004.77 ± 1090.38	6.56 ± 1.08	177.92 ± 47.68
Sandimmun Neoral®	1.83 ± 0.75	969.68 ± 176.30	22.29 ± 10.54	4739.52 ± 806.30	5462.31 ± 990.76	6.39 ± 0.70	

Note: *Calculated on $AUC_{0-\infty}$ with Sandimmun Neoral® as reference.

Table 3 Pharmacokinetic parameters after oral administration of CyA-loaded cubic nanoparticles and Sandimmun Neoral® calculated by a two-compartmental method

Formulation	k_a (h^{-1})	α (h^{-1})	β (h^{-1})	$t_{1/2(\alpha)}$ (h)	$t_{1/2(\beta)}$ (h)	$t_{1/2(a)}$ (h)	k_{10} (h^{-1})	k_{12} (h^{-1})	k_{21} (h^{-1})
Cubic nanoparticles	0.52 ± 0.076	0.24 ± 0.068	0.062 ± 0.056	3.05 ± 0.90	12.14 ± 8.37	1.46 ± 0.37	0.096 ± 0.047	0.081 ± 0.10	0.13 ± 0.10
Sandimmun Neoral®	0.73 ± 0.37	0.41 ± 0.12	0.032 ± 0.022	1.84 ± 0.57	22.29 ± 10.54	1.14 ± 0.61	0.10 ± 0.054	0.19 ± 0.10	0.14 ± 0.17

Comparing the pharmacokinetic parameters and oral bioavailability data indicates the effects of cubic nanoparticles on the oral absorption of CyA. Although the significance of the cubic structure of the nanoparticles on enhanced absorption has not been elucidated at this stage of study, there are a few assumptions regarding the merits of cubic nanoparticles as potential oral drug delivery carriers. Studies by Um and colleagues[28] confirmed that both released drugs or cubic nanoparticle-associated drugs can be transported across the endothelial cell membranes enhancing drug absorption. Whether or not cubic nanoparticles can be transported intact across cell membranes has yet to be determined however, they are known to possess lyotropic properties. This property makes it easier for nanoparticles to penetrate the "unstirred water layer"[21,34,35] and make closer contact with cell membranes. This may promote their uptake by endothelial membranes although this has yet to be tested experimentally. It has to be stressed however, that the transportation of cubic nanoparticles across cell membranes is not the only mechanism by which they may improve drug absorption as compared to orally administered lipid carriers. In previous studies with GMO liquid-crystalline phase oral formulation, digestion of the matrix by intestinal esterase to form lyotropic nanostructures was proposed as the main mechanism to enhance the oral bioavailability of the incorporated drugs.[36] Oleyl glycerate (OG) matrices showed slower digestion rate than GMO, which was attributable to the significant enhancement in oral bioavailability and extended absorption profile for a few days.[37] It can also be assumed that cubic nanoparticles will also be digested in the GI and broken down into smaller nanoparticles or drug-associated micelles. One advantage of cubic nanoparticles is that they are isotropic and fragmentation only results in the formation of smaller cubic nanoparticles that retain the properties of their "parental" nanoparticles. Here, the secondary cubic nanoparticles or derivative vehicles like micelles may facilitate further contact with cell membrane and facilitate absorption. Recent work on liquid crystalline matrix based on phytantriol indicated that the nanostructure of these materials might provide the ability to tailor the release rate and oral absorption kinetics of hydrophilic drugs.[38]

It seems that multiple mechanisms, rather than a single mechanism, including transportation of cubic nanoparticles across cell membranes, enhanced contact with cell surfaces and enhanced absorption through the lipid digestion process may contribute to enhanced oral bioavailability of CyA.

Conclusions

The results of this study indicated that cubic nanoparticles were superior to microemulsion-based formulation in improving the oral bioavailability of CyA. The oral bioavailability of CyA cubic nanoparticles were enhanced significantly to approximately 178% as compared to Sandimmun Neoral®.

Acknowledgments

This work was supported by National Key Basic Research Program of China (2007CB935800, 2009CB930300) and partly by the Ministry of Education (200802461092). We thank Dr Kunpeng Li of Zhongshan University for help with Cryo-TEM analysis and Dr Jianming Chen of the Second Military Medical University for help with particle size measurements. The authors report no conflicts of interest in this work.

References

1. Dunn CJ, Wagstaff AJ, Perry CM, et al. Cyclosporin: an updated review of the pharmacokinetic properties, clinical efficacy and tolerability of a microemulsion-based formulation (Neoral®) in organ transplantation. *Drugs*. 2001;61:1957–2016.
2. Hebert MF. Contributions of hepatic and intestinal matabolism and Pglycoprotein to cyclosporin ans tacrolimus oral drug delivery. *Adv Drug Deliv Rev*. 1997;27:201–214.
3. Tjai JF, Webber IR, Back DJ. Cyclosporin metabolism by the gastrointestinal mucosa. *Br J Clin Pharmacol*. 1991;31:344–346.
4. Noble S, Markham A. Cyclosporin: a review of the pharmacokinetic properties, clinical efficacy and tolerability of a microemulsion-based formulation (Neoral®). *Drugs*. 1995;50:924–941.
5. Vonderscher J, Meinzer A. Rationale for the development of Sandimmun Neoral. *Transplant Proc*. 1994;26:2925–2927.
6. Mueller EA, Kovarik JM, van Bree JB, et al. Improved dose linearity of cyclosporine pharmacokinetics from a microemulsion formulation. *Pharm Res*. 1994;11:301–304.
7. Dai J, Nagai T, Wang X, et al. pH-sensitive nanoparticles for improving the oral bioavailability of cyclosporine A. *Int J Pharm*. 2004;280:229–240.

8. Wang XQ, Dai JD, Chen Z, et al. Bioavailability and pharmacokinetics of cyclosporine A-loaded pH-sensitive nanoparticles for oral administration. *J Control Release*. 2004;97:421–429.
9. Wang XQ, Huang J, Dai JD, et al. Long-term studies on the stability and oral bioavailability of cyclosporine A nanoparticle colloid. *Int J Pharm*. 2006;322:146–153.
10. Italia JL, Bhatt DK, Bhardwaj V, et al. PLGA nanoparticles for oral delivery of cyclosporine: nephrotoxicity and pharmacokinetic studies in comparison to Sandimmun Neoral. *J Control Release*. 2007;119: 197–206.
11. El-Shabouri MH. Positively charged nanoparticles for improving the oral bioavailability of cyclosporin-A. *Int J Pharm*. 2002;249:101–108.
12. Müller RH, Runge S, Ravelli V, et al. Oral bioavailability of cyclosporine: solid lipid nanoparticles (SLN) versus drug nanocrystals. *Int J Pharm*. 2006;317:82–89.
13. Aliabadi HM, Brocks DR, Lavasanifar A. Polymeric micelles for the solubilization and delivery of cyclosporine A: pharmacokinetics and biodistribution. *Biomaterials*. 2005;26:7251–7259.
14. Guo J, Wu T, Ping Q, et al. Solubilization and pharmacokinetic behaviors of sodium cholate/lecithin-mixed micelles containing cyclosporine A. *Drug Deliv*. 2005;12:35–39.
15. Lee EJ, Lee SW, Choi HG, et al. Bioavailability of cyclosporin A dispersed in sodium lauryl sulfate-dextrin based solid microspheres. *Int J Pharm*. 2001;218:125–131.
16. Guo J, Ping Q, Chen Y. Pharmacokinetic behavior of cyclosporin A in rabbits by oral administration of lecithin vesicle and Sandimmun Neoral. *Int J Pharm*. 2001;216:17–21.
17. Shah NM, Parikh J, Namdeo A, et al. Preparation, characterization and in vivo studies of proliposomes containing Cyclosporine A. *J Nanosci Nanotechnol*. 2006;6:2967–2973.
18. Liu C, Wu J, Shi B, et al. Enhancing the bioavailability of cyclosporine a using solid dispersion containing polyoxyethylene (40) stearate. *Drug Dev Ind Pharm*. 2006;32:115–123.
19. Chen MC, Wang JL, Tzen JT. Elevating bioavailability of cyclosporine a via encapsulation in artificial oil bodies stabilized by caleosin. *Biotechnol Prog*. 2005;21:1297–1301.
20. Kim SJ, Choi HK, Lee YB. Pharmacokinetic and pharmacodynamic evaluation of cyclosporin A O/W-emulsion in rats. *Int J Pharm*. 2002;249:149–156.
21. Thomson AB, Schoeller C, Keelan M, et al. Lipid absorption: passing through the unstirred layers, brush-border membrane, and beyond. *Can J Physiol Pharmacol*. 1993;71:531–555.
22. Porter CJ, Trevaskis NL, Charman WN. Lipids and lipid-based formulations: optimizing the oral delivery of lipophilic drugs. *Nat Rev Drug Discov*. 2007;6:231–248.
23. Barauskas J, Johnsson M, Tiberg F. Self-aseembled lipid supersture beyond vesicles and liposomes. *Nano Lett*. 2005;5:1615–1619.
24. Yang D, Armitage B, Marder SR. Cubic liquid-crystalline nanoparticles. *Angew Chem Int Ed*. 2004;43:4402–4409.
25. Esposito E, Cortesi R, Drechsler M, et al. Cubosome dispersions as delivery systems for percutaneous administration of indomethacin. *Pharm Res*. 2005;22:2163–2173.
26. Garg G, Saraf S, Saraf S. Cubosomes: an overview. *Biol Pharm Bull*. 2007;30:350–353.
27. Chung H, Kim J, Um JY, et al. Self-asembled "nanocubicle" as a carrier for peroral insulin delivery. *Diabetologia*. 2002;45:448–451.
28. Um JY, Chung H, Kim KS, et al. In vitro cellular interaction and absorption of dispersed cubic particles. *Int J Pharm*. 2003;253: 71–80.
29. Lai J, Chen J, Lu Y, et al. Glyceryl monooleate/poloxamer 407 cubic nanoparticles as oral drug delivery systems: I. In vitro evaluation and enhanced oral bioavailability of the poorly water-soluble drug simvastatin. *AAPS PharmSciTech*. 2009;10:960–966.
30. Gustafsson J, Ljusberg-Wahren H, Almgren M. Cubic lipid-water phase dispersed into submicron particles. *Langmuir*. 1996;12:4611–4613.
31. Jin Y, Ai P, Xin R, et al. Morphological transformation of self-assembled nanostructures prepared from cholesteryl acyldidanosine and the optimal formulation of nanoparticulate system: Effect of solvents, acyl chain length and poloxamer 188. *J Colloid Interf Sci*. 2008;326:275–282.
32. Missirlis D, Kawamura R, Tirelli N, et al. Doxorubicin encapsulation and diffusional release from stable, polymeric, hydrogel nanoparticles. *Eur J Pharm Sci*. 2006;29:120–129.
33. Chimalakonda AP, Shah RB, Mehvar R. High-performance liquid chromatographic analysis of cyclosporin A in rat blood and liver using a commercially available internal standard. *J Chromatogr B*. 2002;772:107–114.
34. Katneni K, Charman SA, Porter CJ. An evaluation of the relative roles of the unstirred water layer and receptor sink in limiting the in-vitro intestinal permeability of drug compounds of varying lipophilicity. *J Pharm Pharmacol*. 2008;60:1311–1319.
35. Korjamo T, Heikkinen AT, Mönkkönen J. Analysis of unstirred water layer in in vitro permeability experiments. *J Pharm Sci*. 2009;98: 4469–4479.
36. Boyd BJ, Whittaker DV, Khoo SM, et al. Lyotropic liquid crystalline phases formed from glycerate surfactants as sustained release drug delivery systems. *Int J Pharm*. 2006;309:218–226.
37. Boyd BJ, Khoo SM, Whittaker DV, et al. A lipid-based liquid crystalline matrix that provides sustained release and enhanced oral bioavailability for a model poorly water soluble drug in rats. *Int J Pharm*. 2007;340:52–60.
38. Lee KW, Nguyen TH, Hanley T, et al. Nanostructure of liquid crystalline matrix determines in vitro sustained release and in vivo oral absorption kinetics for hydrophilic model drugs. *Int J Pharm*. 2009;365: 190–199.